AD NUMBER
AD508283
CLASSIFICATION CHANGES
TO: unclassified
FROM: confidential
LIMITATION CHANGES
TO: Approved for public release, distribution unlimited
FROM: Distribution authorized to U.S. Gov't. agencies and their contractors; Administrative/Operational Use; FEB 1970. Other requests shall be referred to Air Force Cambridge Research Laboratories, Attn: CRF, Hanscom Field, Bedford MA 01730.
AUTHORITY
OL-AA PL/GPS, ltr, 8 Nov 1995; OL-AA PL/GPS, ltr, 8 Nov 1995

AD NUMBER

AD508283

CLASSIFICATION CHANGES

TO

confidential

FROM

secret

AUTHORITY

28 Feb 1982, per document marking, DoDD 5200.10

SECURITY MARKING

The classified or limited status of this report applies to each page, unless otherwise marked.
Separate page printouts MUST be marked accordingly.

THIS DOCUMENT CONTAINS INFORMATION AFFECTING THE NATIONAL DEFENSE OF THE UNITED STATES WITHIN THE MEANING OF THE ESPIONAGE LAWS, TITLE 18, U.S.C., SECTIONS 793 AND 794. THE TRANSMISSION OR THE REVELATION OF ITS CONTENTS IN ANY MANNER TO AN UNAUTHORIZED PERSON IS PROHIBITED BY LAW.

NOTICE: When government or other drawings, specifications or other data are used for any purpose other than in connection with a definitely related government procurement operation, the U.S. Government thereby incurs no responsibility, nor any obligation whatsoever; and the fact that the Government may have formulated, furnished, or in any way supplied the said drawings, specifications, or other data is not to be regarded by implication or otherwise as in any manner licensing the holder or any other person or corporation, or conveying any rights or permission to manufacture, use or sell any patented invention that may in any way be related thereto.

AD- 508283

SECURITY REMARKING REQUIREMENTS

DOD 5200.1-R, DEC 78

REVIEW ON 28 FEB 90

SECRET

AFCRL-70-0094
FEBRUARY 1970
AIR FORCE SURVEYS IN GEOPHYSICS, NO. 215

AIR FORCE CAMBRIDGE RESEARCH LABORATORIES
L. G. HANSCOM FIELD, BEDFORD, MASSACHUSETTS

(U) Aerial Magnetic Detection in Counter-Insurgency Warfare Part II, Experimental Results

E.J. ZAWALICK, LT COL, USAF, RETIRED
R.O. HUTCHINSON

OFFICE OF AEROSPACE RESEARCH
United States Air Force

SECRET

SECRET

AFCRL-70-0096
FEBRUARY 1970
AIR FORCE SURVEYS IN GEOPHYSICS, NO. 215

SPACE PHYSICS LABORATORY PROJECTS 7601,8601

AIR FORCE CAMBRIDGE RESEARCH LABORATORIES

L. G. HANSCOM FIELD, BEDFORD, MASSACHUSETTS

(U) Aerial Magnetic Detection in Counter-Insurgency Warfare Part II, Experimental Results

E.J. ZAWALICK, LT COL, USAF, RETIRED
R.O. HUTCHINSON

OFFICE OF AEROSPACE RESEARCH
United States Air Force

SECRET

Abstract

(U) Component gradiometer and total intensity magnetometer systems performances for use in aerial magnetic detection were compared. Permanent and induced fields and resultant magnetic moments and the ranges of variations for target vehicles were obtained. Dynamic signatures from these same vehicles were obtained with a modified commercial magnetometer. The total field system was installed in a Grumman Tracker (S2E) aircraft and a joint program with the Naval Air Development Center, Johnsville, Pa., resulted in a series of flight tests over various combinations of target size, spacing, heading, and geologic conditions. Analytical expressions were derived for target signatures and showed good agreement with experimental values. Application of the observed results to specific areas within Southeastern Asia and their associated geologic noise spectra is discussed.

Contents

Illustrations

Tables

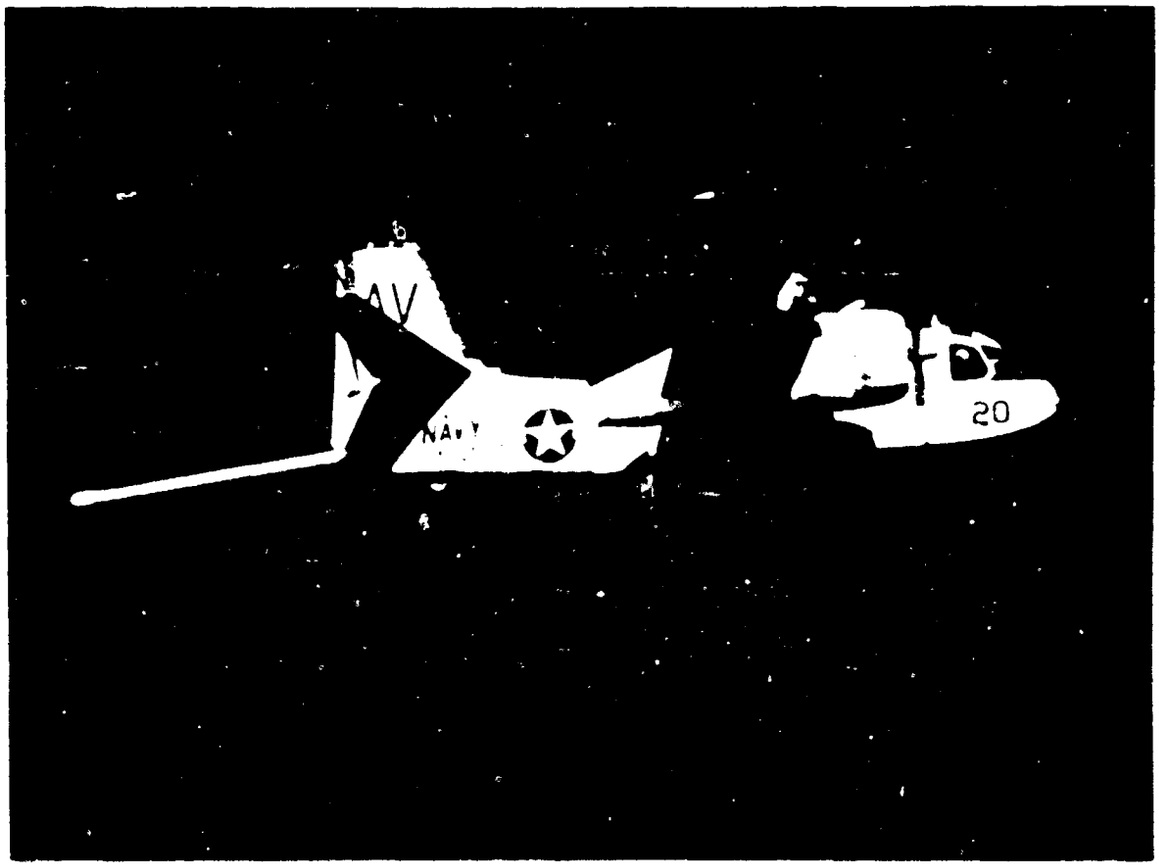

Grumman Tracker (S2E) Aircraft with MAD Boom Extended

Aerial Magnetic Detection in Counter-Insurgency Warfare – Part II, Experimental Results (U)

1. INTRODUCTION

(U) The general applicability of aeromagnetic detection techniques to counter-insurgency warfare was outlined by Maple (1966) in a preliminary technical paper. The specific operational usefulness of such a system depends on the sensitivity of the magnetic detector, the magnitude of the target field, and the available signal-to-noise ratio of the detection system in the area in which deployed. This report examines each of these factors, in turn, with special emphasis on the collection and interpretation of experimental data and the applicability of the observed results to present limited warfare operations.

(U) One of the first military uses of aeromagnetic detection was the Navy's attempt to locate enemy submarines during World War II. The magnetic airborne detection (MAD) system developed for this purpose used a tri-axial, self-orienting, fluxgate and could obtain useable signals at distances of a few hundred feet. Improvements in sensor electronics, reduction in aircraft magnetic noise levels, and increases in size of most target submarines have provided considerable increases in detection range.

(U) Current detector studies and their proposed future programs call for the replacement of fluxgate units with optically pumped gaseous sensors. Results of

(Received for publication 5 December 1969)

this Navy development program and of AFCRL's program to provide lightweight highly sensitive, magnetic detectors for rocket and satellite payloads have been combined and extended to land target operations. It should be noted, however, that despite overall improvements in sensor performance and in survey aircraft noise levels, detection of COIN targets is made difficult by their relatively small size and by the increased background geologic induced, magnetic noise against which they must be found.

2. SENSOR DEVELOPMENT

(U) Two types of highly sensitive field measuring devices are considered in detail. The results of these studies follow.

2.1 Component Gradiometer

(U) An extensive study to determine the feasibility of a portable component magnetic gradiometer was performed by Flannery et al. (1967). Variable-mu magnetometer elements were combined to form a stationary gradiometer and signatures obtained from targets of interest.

(U) Figure 1 shows two recordings of the system's response to a van-type vehicle at varying distances from the detector. The upper recording is the gradiometer output; the lower is a record of a single sensor output. This record shows the dependence of output on not only distance but also on the direction of travel of the vehicle. System bandwidth was 0.1 Hz to 40 Hz. Both recordings show high noise levels: 750 milligammas for the single sensor and 250 milligammas for the gradiometer output. Since the gradient varies inversely as the fourth power of the distance, it follows that the signal at 192 feet will be one-sixteenth of that at 96 feet. It is evident from Figure 1 that the target signal would be smaller than the noise; therefore, the target would not be detected at distances of 200 feet or more.

(U) The gradiometer tested was constructed from a modified three-component magnetometer built by the Electro-Mechanics Company (EMCO) of Austin, Texas. Its overall performance was not comparable to other gradiometers built by EMCO due mostly to excessive system noise. The effective noise level of the system could have been reduced somewhat by reducing the effective bandwidth of the system. However, it did not appear that a great improvement in detection range could be readily attained for the stationary gradiometer. Because of this and because of the extensive problems involved in producing a portable device, no further gradiometer hardware development was supported.

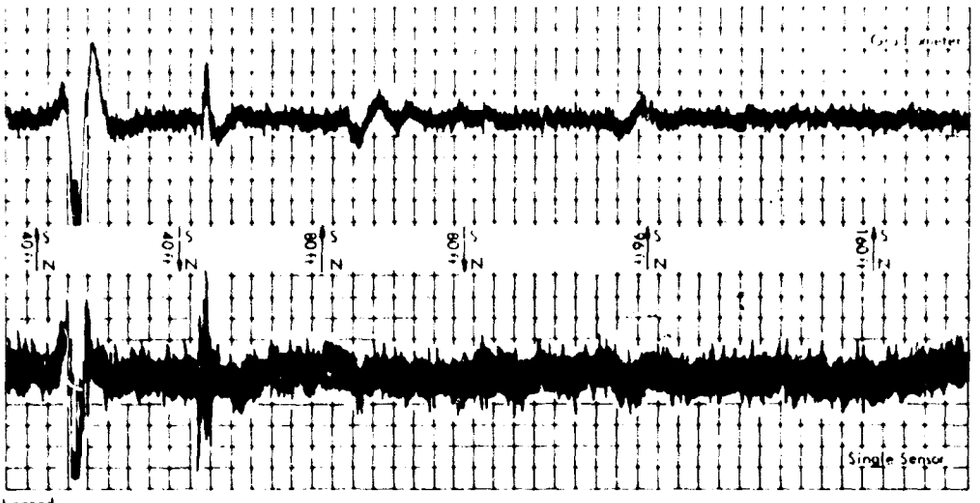

Legend:
Sensor Spacing: 8' 8"
Direction of Travel: N-S, S-N
Response: 0.01 to 40 Hz
Beam Orientation: E-W
Sensor Orientation: E-W

Figure 1. Variable-mu Gradiometer and Magnetometer Response vs. Distance

2.2 Total Intensity Magnetometer

(U) Optically pumped magnetometers have been used successfully in various rocket and satellite payloads to measure small changes in magnetic fields. These self-oscillating instruments are small, have no moving parts, are not generally sensitive to heading errors, and require very little power. Built mostly by Varian Associates, Palo Alto, California, the units use cesium or rubidium vapor as a working fluid.

(U) An airborne reconnaissance magnetometer system (ARMS) was built to AFCRL specifications by Varian and delivered for evaluation as a flight prototype. The sensor, a six-cell, single-lamp, cesium vapor, optically-pumped unit and the sensor electronics weigh 12.6 lbs. They occupy a cylinder about 7 in. in diameter and 40 in. long. The readout control console and display chassis occupy 16 in. of a standard relay rack and weigh 90 lbs. Figure 2 shows the ARMS sensing head and Figure 3 the ARMS control and display units.

(U) The omnidirectional sensor detects the total intensity of the earth's magnetic field, and in conjunction with the sensor electronics, provides an output frequency which is related to the field strength by the cesium 133 gyromagnetic ratio of 3.49 Hz/gamma. The sensor head contains an RF cesium lamp, six cesium resonance cells with H_1 coils, and the necessary optical accessories such as lens, polarizers, filters, and photoelectric detectors. These units are mounted within an

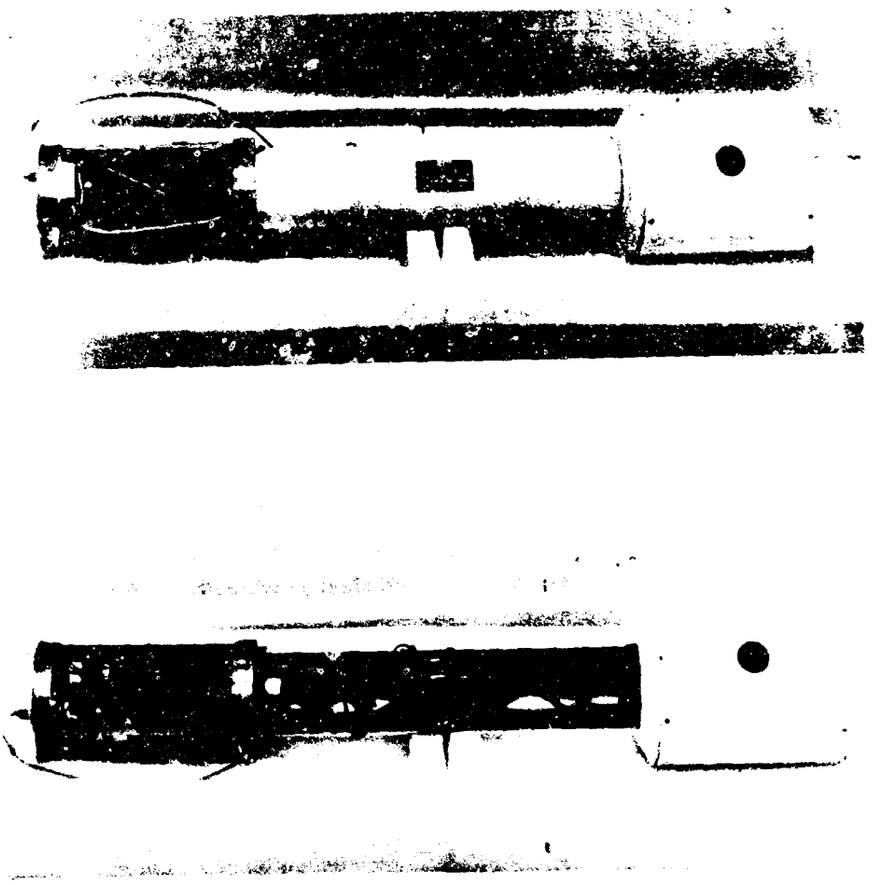

Figure 2. ARMS Sensing Head

insulated temperature controlled package and covered with a conductive coating for RFI shielding. Sensor electronics are located at the opposite end of the sensor cylinder and include six signal preamplifiers, a voltage regulator, RF lamp exciter and regulator, amplifiers, summing circuitry, filters, couplers, and the temperature controller. The package is connected to the control unit through a single, coaxial cable used to supply power to the sensor and to return the magnetometer's Larmor signal.

(U) The control unit contains a power converter, voltage, current, and signal monitors, a frequency-to-voltage discriminator for converting the sensor output frequency to a DC voltage, sweep circuits for the display chassis, and a bandpass

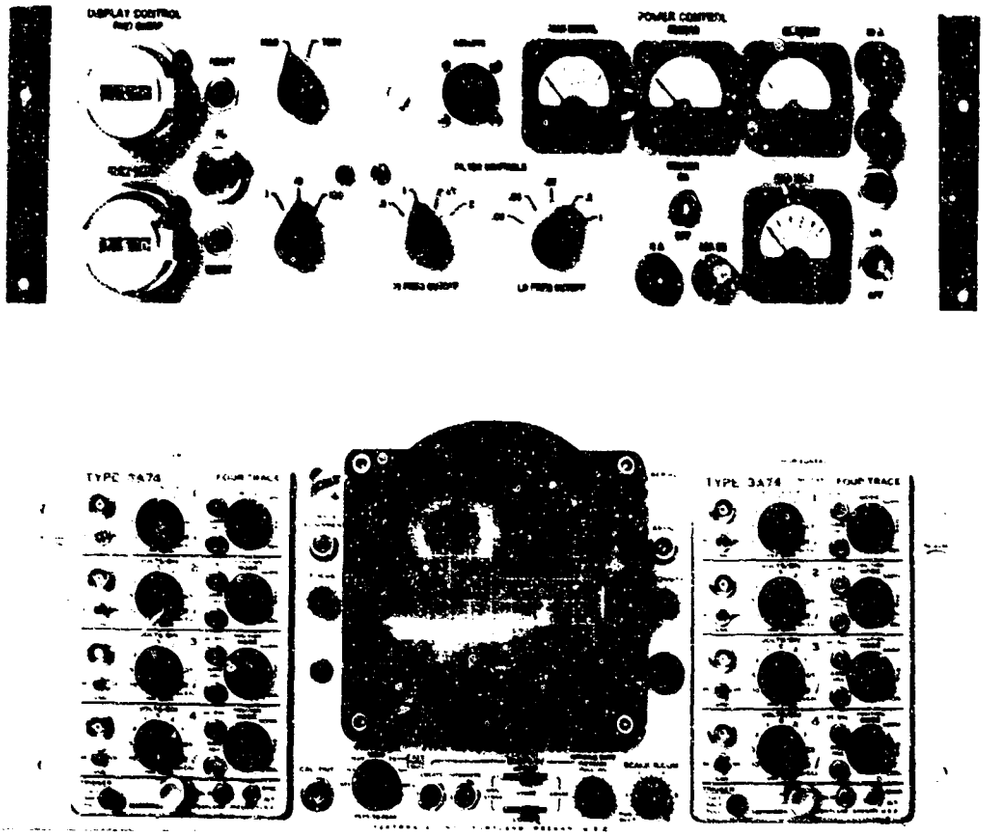

Figure 3. ARMS Control and Display Units

filter. The unit's output, an AC coupled signal, is presented to the display unit at a sensitivity level of one volt per gamma.

(U) The display unit is an adaptation of a Tektronix Model RM 564 Oscilloscope. This is a split-screen storage oscilloscope with independent upper and lower memory control circuits and provisions for manual remote or local erase of either or both of the upper and lower halves of the CRT. Four identical input channels for both vertical and horizontal axes are available. Two channels, one upper and one lower, are used for the MAD signal. Two are spares available for backup or to monitor changes in altitude and/or air speed. Sweep speed on the upper MAD channel is set to correspond to the aircraft's ground speed and to the length of the desired detection run. One sweep of the scope trace from left to right thus covers one pass over a suspected target. The sweep speed of the lower MAD channel is set to a sub-multiple of the upper sweep rate, thus moving from left to right at one tenth to one hundredth of the upper trace. This arrangement permits the operator

to have displayed at any instant the signature of a suspected target plus the results of many passes at various altitudes, headings, or off-sets over the same suspicious area. This information can then be used to localize the target position, estimate target movement, if any, and direct an attack.

(U) Power consumption of the sensor and its controls is about 2.5 amperes at 28 vdc after warmup and the display requires a maximum of 2 amperes at 117 volts, 400 Hz. Normal operating range is from -10°C to +55°C and extended operation for up to several hours is possible at temperatures down to -60°C provided the unit is first operated within its normal range.

(S) Total systems noise is less than 0.005γ for a land target bandpass filter setting of from 0.07 to 0.5 Hz. Roll, pitch and yaw motion noise is less than 0.01γ for 5 degree peak-to-peak excursions in mid and high latitudes increasing to about 0.10γ at the equator. Much of this noise can be removed by suitable filter settings. Additional performance figures and acceptance test data can be obtained from McBride (1967) and McBride (1968).

3. MAGNETIC MOMENTS OF TARGETS

(U) If the distance from the target is large compared with the dimensions of the target, as it will normally be for aerial magnetic detection, the target may conveniently be considered to be a magnetic dipole having an equivalent dipole moment.

(U) The magnetic field, F, of a dipole of moment, M, is given in cgs units by

$$F = (M/r^3)\sqrt{1 + 3\cos^2\theta} \qquad (1)$$

where r is the distance from the dipole and θ is the angle between the direction of the dipole axis and the line from the dipole to the point of measurement. At a given distance from the target, the field thus varies from $2M/r^3$ to M/r^3, the most favorable location being along the axis of the dipole or bar magnet representing the target.

(U) The magnetic moment of a given mass of magnetic material will depend upon its geometrical shape and may vary widely. If the shape is approximated by a cylinder, the larger the L/D (length-to-diameter) ratio, the larger the resulting moment will be. In practice, many targets, such as trucks, will have relatively unfavorable geometrical configurations, and if the equivalent L/D ratios do not vary greatly, the magnetic moment will be approximately proportional to the mass of the magnetic material in the target.

(U) An empirical equation (Fisher, 1966) for horizontal dipole steel targets aligned north and south and valid for Southern Thailand and similar latitudes is

$$S = \frac{133M^{0.76}}{R^3} \qquad (2)$$

where S = signal amplitude in gammas for a north-south traverse,

M = steel mass of target in kilograms

R = distance of nearest approach in meters.

(U) Equation (2) is accurate to about a factor of two for masses from 1 to 6,000 kilograms, and can be used to estimate the minimum mass of steel that can be detected by an airborne magnetometer.

(C) If we assume that the minimum detectable target signal is 0.06 gammas and that the minimum flight altitude is 50 meters it follows from Eq. (1) that the minimum mass of iron in the target must be 200 kilograms or about one fourth of a ton. If the flight altitude is increased to 100 meters or about 330 feet, then the mass of the target must be approximately 4 tons. Field artillery pieces, mortars, and rocket launchers, although much less massive, may also be detectable at considerable distances due to their favorable length-to-diameter ratios.

(U) In order to determine more fully the magnetic signatures of various types of target vehicles as functions of heading velocity and inducing fields, an experimental program of static and dynamic measurements was undertaken.

3.1 Static Measurements

(U) Simplified determinations of the magnetic moments of various objects depend on the assumption that their moments can be represented by a dipole approximation. For the trucks used as our targets, it was necessary to determine at what distance the magnetic field contributions due to higher order multipoles could be neglected.

(U) The basic sensor used for this determination was a model MFO-3SP Fluxgate Magnetometer manufactured by Sharpe Instruments of Canada and employing three mutually orthogonal detector elements. Tests were conducted as follows. The sensing head was set on its tripod at a height corresponding roughly to the height of the center of mass of the truck. The magnetometer was leveled and aligned so that the X-component coincided with magnetic north by rotating about Z until a zero reading was obtained for the Y-component. North-south and east-west magnetic base lines passing through the magnetometer were surveyed and the magnetometer was then enclosed with a wooden shelter to reduce wind loading vibration and tilt effects.

(C) Measurements were made only on those days when magnetic activity was low. It was accomplished by placing the center of the vehicle mass over the desired distance marker aligning as required, reading the three component values,

quickly driving the vehicle away, and then reading the three unbiased earth's field component values. Table 1 shows a typical test sample obtained from a standard 2-1/2 ton Army truck located south of the sensor and facing north at various distances from the sensor. Given values are in gammas and represent the difference between biased and unbiased component values taken at L. G. Hanscom Field. Normal background magnetic field values were H = 16,900γ and Z = 52,500γ.

(C) Table 1. Magnetic Field Components for a 2-1/2 Ton Truck vs. Distance

Distance (feet)	X	Y	Z
60	22.4 ± 2	0	-18.4 ± 0.5
80	9.1 ± 2	0	-8.0 ± 0.5
100	4.8 ± 1	0	-4.0 ± 0.5
120	2.4 ± 0.4	0	-2.5 ± 0.3

(C) Figure 4 is a plot of the above data and shows that the components of the target vehicle vary very much like the theoretical dipole drawn in as a solid line. It can be concluded that a distance of 60 feet is sufficient to insure dipole-like behavior of the truck's field and a large signal for accurate moment determinations. Although magnetic field values are recorded to the nearest 0.1γ it is estimated that the absolute accuracy is not better than ± 1 gamma per component. An example of the reproducibility of experimental results is shown in Table 2. The measurements, also made at L. G. Hanscom Field, include errors caused by instrumental noise and drift and small variations in the positioning of the truck.

(C) The dependence of the induced dipole moment on the direction of the target relative to the inducing magnetic field was investigated. The truck was placed at a fixed distance south of the magnetometer and headed in the cardinal (magnetic) directions while the axes of the sensor remained fixed. The experimental results for five separate 2-1/2 ton Army trucks are presented in Table 3. Dipole moments were calculated from the expression

$$M = r^3\sqrt{\frac{F_x^2}{4} + F_y^2 + F_z^2} \qquad (3)$$

which is valid only for the measurement geometry as described above where the x-axis coincides with magnetic north.

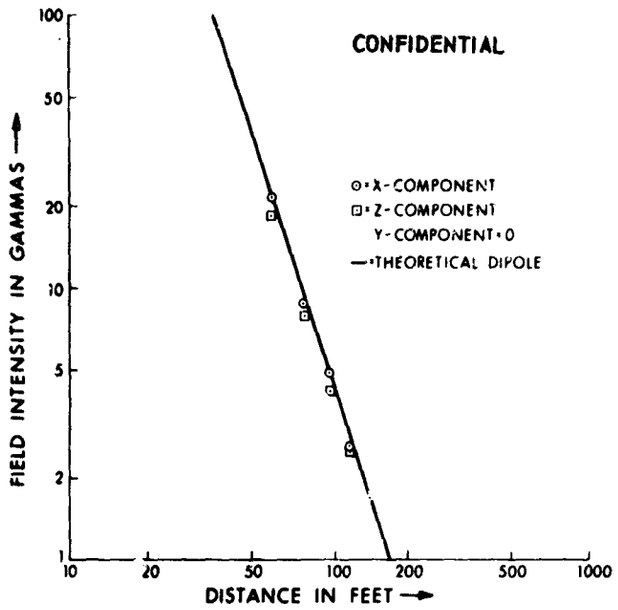

Figure 4. Magnetic Field of a 2-1/2 Ton Truck

(C) Table 2. Reproducibility of experimental measurements of magnetic field of a 2-1/2 ton Army truck in gammas vs. distance in feet. (In all cases, the vehicle was located south of the sensor and was headed north.)

Distance	X-component	Y-component	Z-component
60'	24.5	0	-18.0
	21.0	0.2	-18.0
	21.8	-0.2	-19.0
	22.4	-1.0	-18.7
80'	11.0	0.3	-8.0
	8.6	0.1	-7.6
	9.1	-0.3	-8.2
	8.9	-0.5	-8.2
100'	4.0	-0.6	-3.0
	4.8	0	-4.0
	4.9	0.2	-4.3
120'	2.0	0.5	-2.3
	2.4	0	-2.5
	2.8	-0.2	-2.5

(C) Table 3. Experimental measurement of magnetic fields (in gammas) of five mechanically identical 2-1/2 ton Army trucks vs. vehicle heading. (In all cases, the vehicles were located 60 feet south of the magnetometer.)

Vehicle Heading	X Component	Y Component	Z Component	Total Field	Dipole Moment
North	17.0	1.0	-15.5	23.0	1.08×10^6
South	11.0	2.0	-21.0	23.8	1.33×10^6
East	7.0	-1.0	-17.5	18.9	1.09×10^6
West	8.0	2.5	-17.8	19.7	1.13×10^6
				Average	1.16×10^6
North	21.0	1.0	-16.5	26.7	1.19×10^6
South	7.5	1.0	-22.5	23.7	1.39×10^6
East	8.5	-4.0	-19.2	22.4	1.23×10^6
West	11.5	3.0	-19.0	22.4	1.23×10^6
				Average	1.26×10^6
North	16.5	1.0	-17.5	24.1	1.18×10^6
South	10.0	-1.0	-19.0	21.5	1.20×10^6
East	10.0	1.0	-18.5	21.1	1.17×10^6
West	7.0	-0.5	-18.8	20.1	1.17×10^6
				Average	1.18×10^6
North	16.5	0.0	-18.3	24.6	1.23×10^6
South	10.1	0.0	-19.8	22.2	1.25×10^6
East	8.5	-2.0	-18.0	20.0	1.14×10^6
West	9.4	2.1	-19.0	21.3	1.20×10^6
				Average	1.21×10^6
North	22.4	-1.0	-18.7	29.3	1.33×10^6
South	11.5	0.2	-21.7	24.6	1.37×10^6
East	6.2	9.5	-18.2	21.4	1.27×10^6
West	10.2	3.8	-19.2	22.1	1.24×10^6
				Average	1.30×10^6
	5 Vehicle Average				1.22×10^6

(C) As would be expected from their geometric shape, the magnetization of the trucks in the longitudinal direction (for example, along the length which is the

greatest dimension) is greater than that in the transverse direction. The fact that the vertical magnetization is greater than that in the longitudinal direction (although the vertical dimension is smaller) is due to the large vertical component of the earth's field at this latitude. Since the trucks do not change their oreintation with respect to the vertical inducing field, mechanical vibration during operations results in appreciable permanent magnetization adding to the induced magnetization.

(C) If the fields due to the induced and permanent parts of the longitudinal magnetization add on a north heading, they will subtract for a south heading. The effect of the induced magnetization is therefore obtained by taking half of the sum of the two x-component measurements, while the effect of the permanent magnetization is obtained by taking half of the difference of the two. From Table 3 we find that for the average of the 5 trucks the induced longitudinal magnetization produces an x-component field of about 14 gammas at 60 feet while the permanent longitudinal magnetization produces a field of about 5.5 gammas.

(C) Similarly, from the x-component readings for east and west headings, we find that the induced transverse magnetization produces a field of about 8.5 gammas at 60 feet while the permanent transverse magnetization produces a field of about 1 gamma. The measurements do not permit a separation of the vertical magnetization into induced and permanent parts.

(C) The y-component fields for east and west headings also measure the permanent longitudinal magnetization. Their difference should be half the difference of the x-component measurements for north and south headings. The smaller numbers accentuate the effects of experimental error, but there is general agreement except for the last truck in Table 3 where a major discrepancy appears. This could be due to an error in recording the y-component fields. The y-component readings for north and south headings only confirm a small value of permanent transverse magnetization.

(C) The fields of the trucks will be proportional to the inducing fields. At a low magnetic latitude, the horizontal component of the earth's field could be up to almost twice as large as that at Hanscom Field while the vertical component would be much smaller (zero at the magnetic equator). The horizontal magnetization of the trucks would increase accordingly while the vertical magnetization could be very small.

(C) In the present measurements, the large vertical component of the inducing field should be considered in interpreting the results since it can produce a horizontal component of magnetization (as, for example, in the case of an iron bar inclined at an angle to the vertical). However, since the orientation of the vertical field with respect to the truck does not change, the orientation of the magnetization due to the vertical field will also remain constant with respect to the truck. Any

horizontal magnetization due to the vertical component of the earth's field will therefore appear to be permanent magnetization as far as the x- and y-component measurements are concerned.

(C) The induced magnetization of the trucks in the longitudinal and transverse directions measured at Hanscom Field may be considered representative of the local horizontal inducing field and may be extrapolated to other latitudes. The permanent magnetization in these directions, however, are probably due to the vertical component of inducing field. This could account for the fact that the permanent longitudinal magnetization was in the same direction, toward the front of the truck, for all five cases.

(C) It was also observed that the center of magnetism for the x-component field measurements was at slightly different location than that of the z-component field measurements. If the vehicle heading is kept constant, and if the reference point within the vehicle is correctly chosen, then one should obtain the same field measurements when the vehicle is positioned equidistantly both north and south of the magnetometer. In practice, the reference point was adjusted so that equal horizontal field measurements would result. This produced a small inequality in the z-component measurements which showed that the center of action for the z-component was located more toward the rear of the truck than that of the x-component. These observed differences become insignificant at normal aeromagnetic detection altitudes and are of no consequence for operation in Southeastern Asia where the inducing field is almost entirely horizontal.

3.2 Dynamic Measurements

(U) Dynamic signatures were obtained by driving the trucks past stationary magnetometers making passes along north-south and east-west lines.

(U) Two basic vehicle types were used for these tests: a commercial 1/2-ton pickup truck weighing about 3100 lbs and a 3/4-ton Army weapons carrier weighing about 5800 lbs. Figure 5 shows the unfiltered component field of a 3/4-ton Army truck driven past the Sharpe magnetometer along a south-to-north line 40 feet west of the detector. Tables 4 (1/2-ton) and 5 (3/4-ton) show the results obtained from a total intensity magnetometer for east and west passes under various conditions. Distance refers to closest approach of the truck to the nearest sensor and table entries represent averages of east and west runs. Ranges of variations are shown only when greater than 25 percent. Frequency was obtained by measuring the period of a half wave approximation to the shape of the deflection, doubling its value, and obtaining the reciprocal.

(U) Signal-to-noise (S/N) refers to the ratio of maximum signal amplitude (peak-to-peak) to the total noise (recorder-trace variations measured peak-to-peak).

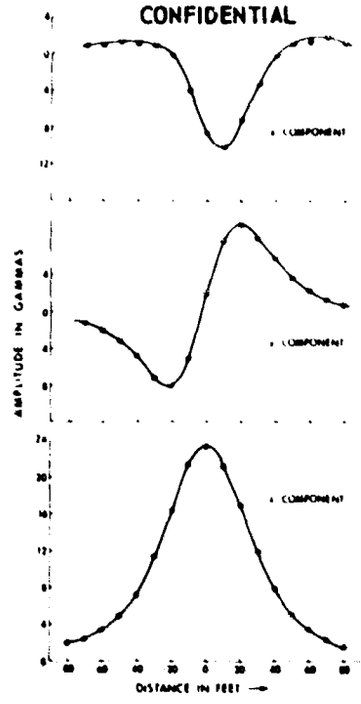

Figure 5. Component Magnetic Field, 3/4-Ton Truck

(C) Table 4. Signal Amplitude, Frequency and Signal to Noise Ratio vs. Distance, Velocity, and Filter Settings for a 1/2-Ton Truck

Dist. (ft.)	Vel. (mph)	Sensors	Filter (Hz)	Amp. (γ)	Freq. (Hz)	S/N
100	30	1	none	1.5	0.08±.02	15
100	30	1	.02-2.0	1.0	0.09	18
135	30	1	.02-2.0	0.7	0.08	15
150	30	1	.02-2.0	0.5±0.2	0.06	5 to 10*
175	30	1	.02-9.0	0.3±0.1	0.06	1?
200	30	1	.05-2.0	0.1	0.05	1.5*
200	30	2	none	0.1	0.07	4
200	30	2	.02-2.0	0.07	0.08	15
200	60	2	none	0.1	0.12	4
200	60	2	.02-2.0	0.06	0.12	10
250	30	2	none	0.05	0.06	3
250	60	2	none	0.04	0.12	3
250	45	2	.02-0.5	0.08	0.08	4

*Results occasionally confused when background noise spectrum varies in and out of range of signal spectrum.

(C) Table 5. Signal Amplitude, Frequency and Signal to Noise Ratio vs. Distance, Velocity, and Filter Settings for a 3/4-Ton Truck

Dist. (ft)	Vel. (mph)	Sensors	Filter (Hz)	Amp. (γ)	Freq. (Hz)	S/N
250	30	2	.03-0.3	0.09	0.04	6
250	45	2	.025-0.25	0.08	0.05	6
250	45	2	.02-0.25	0.09	0.05	7
300	45	2	.03-0.10	0.05	0.04	2+
300	45	2	.02-0.10	0.06	0.04	3
300	60	2	.02-0.10	0.06	0.04	3+

(U) The total intensity sensing system used was a Varian model V-4938-GBF. It consisted of a standard V-4938 rubidium vapor magnetometer, a Brush 4215-10 preamplifier, a Krohn-Hite 330 B filter, and a specially modified Brush Recorder Model mark 250. The basic system sensitivity was 0.01 gamma with a frequency response from DC to 10 Hz. When the bandpass filter was used, the frequency response was limited by the settings of the upper and lower cutoff frequencies shown in Tables 4 and 5. The response outside the pass band was attenuated at 24 db/octave.

(U) Initial system tests showed a high level of magnetic noise within the pass band of interest. This was traced to the operation of high power electronic devices on and around the base, to the city transit system with its high voltage DC system, and to natural noise. Satisfactory operation was obtained by using a second sensing element at some distance from the first sensor, mixing, discriminating, filtering, and displaying the resultant. It should be noted that this does not constitute a gradiometer system. The separation between the two sensors is many times greater than the target to nearest sensor distance. The second sensor serves only as a means of reducing local artificial and natural ionospheric disturbances. Use of the second sensor is denoted by the figure 2 in the sensor column of Tables 4 and 5.

(C) All runs were made along an east-west taxiway located on the north side of Hanscom Field with the magnetometer located at various distances to the north of the taxiway and the recorder in an instrumentation trailer about 1000 feet to the north.

(C) For small target fields, the total field magnetometer measures only that component of the target field which is parallel to the very much larger background field of the earth. At Bedford, where the inclination of the field is about 70 degrees, the total field results are most comparable to the z-component readings of Table 3 and are due chiefly to the vertical magnetization of the truck. At this latitude, the total field readings above the truck would be about twice as large as those in Tables 4 and 5.

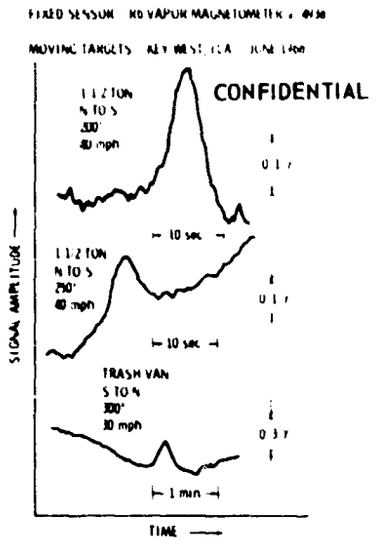

Figure 6. Dynamic Signatures for Various Targets and Fixed Sensor

(C) In South Vietnam, the horizontal field is about twice that at Bedford while the vertical field is small. The induced longitudinal or transverse magnetization of the truck on north-south or east-west headings, respectively, would be correspondingly increased. The vertical magnetization would be small. At that latitude, a total field magnetometer above the truck would be in a less favorable position than one on the ground on the axis of the truck. Judging from the results of Table 3, the detection distances indicated by Tables 4 and 5 would be appreciably increased for airborne detection of the truck on a north-south heading in Vietnam but decreased somewhat for east-west headings. Figure 6 shows the results of such tests performed at Key West, Florida, in an area where the horizontal inducing field is about 26,000γ. Magnetometer bandpass was DC to 20 Hz and the sensor was located to the east of the road.

(C) It may be concluded that with relative target-sensor velocities of 60 mph and proper filtering, a target the size of a 3/4-ton truck can be positively identified at a distance of 300 feet in mid-latitudes. Secondly, that this range can be increased moderately by more favorable horizontal field values and orientations, by increased relative target speeds, and by sharper filter characteristics.

4. GEOLOGIC CONSIDERATIONS

(C) The effectiveness of aeromagnetic detection for COIN warfare in Southeastern Asia is limited primarily by the magnetic relief of the areas in question rather than by any consideration of instrumental sensitivities. This natural

magnetic noise is a result of changes in magnetic susceptibility as functions of topography, soil material, and underlying bedrock geology and is primarily dependent on the manner of dissemination of the mineral magnetite, Fe_3O_4 in these materials.

(U) Direct measurements of this noise spectrum in many parts of Southeastern Asia would be either very hazardous or politically impossible, but studies of areas in the United States that are analogous to certain areas in Southeastern Asia (SEA) have been completed by Curtis (1966). Selection criteria included surface form, surface materials (soils), geology, vegetation, and drainage characteristics. Table 6 shows areas in the United States analogous to areas of SEA in terms of geology and geography as sources of magnetic noise.

(U) Table 6. Geologic Noise Study

Southeastern Asia	United States Equivalent
Southwestern Cambodian Coast Vietnam Coast between the Mekong and Red Rivers Tonkin Coast of North Vietnam	Southern Georgia Coastal Plain
Khorat Plateau of Northeastern Thailand and Western Laos	South Central Georgia
Chaine Annamitique of Central and Southern Laos, Southern Portion of North Vietnam, the Northern Portion of South Vietnam and Eastern Cambodia	Southern Blue Ridge Area of the Appalachians (Tennessee, North Carolina Border)
Highland Plateau Areas of Chaine Annamitique (Pleiku and Dak Song)	Appalachian Piedmont of North Carolina
Mekong and Red River Deltas	Mississippi Delta of Louisiana
Inland River Plains of Thailand and Cambodia and Areas of the Red River in North Vietnam near Hanoi	Alluvial Plains Section of the Mississippi River from Baton Rouge, La., to Natchez, Miss.

(S) A limited amount of experimental data was obtained in South Vietnam. Passes were made with a total intensity magnetometer over shallow coastal waters, several small islands, and portions of the mainland in an area of strong geologic contrasts including granitic intrusives and marine sediments. Figure 7 shows the frequency distribution of magnetic noise at a flight altitude of 440 feet. Note that the dipole target frequency is considerably higher than the peak magnetic noise frequency. This condition was also evident at lower altitudes.

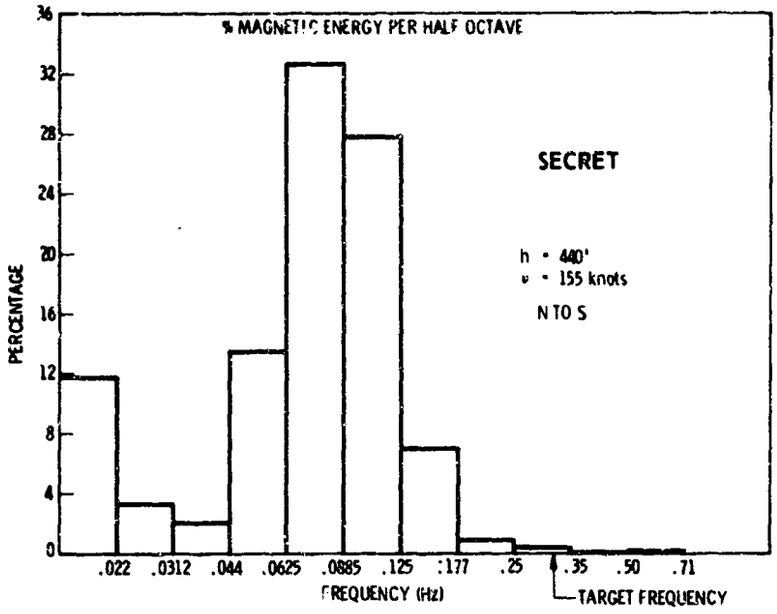

Figure 7. Geologic Noise Spectrum, South Vietnam Coast Region

5. FLIGHT TEST PROGRAM

(U) The range of any aeromagnetic detection system depends on the target size (total magnetic moment), sensor sensitivity, the noise environment, and the relative target-detector velocity. The military applicability of such systems also depends on the simplicity of the operating controls and the display system. Factors concerned with or affected by aircraft are considered in this section and actual test results presented.

5.1 Aircraft Considerations

(U) A total intensity magnetometer responds only to the amplitude of the magnetic field that it is sensing and therefore is ideally suited for use aboard an aircraft. However, any aircraft has associated with it permanent and DC current-type fields plus induced magnetic fields that vary as a function of heading. Using the available sensitivity of any magnetometer system requires mounting the sensor at some distance from the aircraft or compensating for the aircraft's magnetic effects or a combination of both.

(C) Magnetometers have been mounted in streamlined housings called "birds" and towed behind aircraft. A cable and winch system is required and problems have been encountered with "bird" stability and with retrieval operations. A number of

SECRET
(This page is confidential)

"birds" have been lost when the towing aircraft or helicopter was engaged in low level or terrain clearance flights. Best results have been obtained using an extendable boom or "stinger" mounted aft under the tail section and a nine term compensator for further reduction of the aircraft's fields.

(C) An attempt to select an Air Force aircraft in which to test the magnetometer system, developed specifically for COIN applications, was unsuccessful. There are no current operational aircraft that are specifically constructed to minimize magnetic fields or have provisions for an extendable non-magnetic boom or which have an internal compensation system. A previous compensation (McClay and Shuman, 1955) shows that it is possible to modify military aircraft for use as magnetometer platforms but it was both extremely costly and extremely time-consuming. Hence, no such effort was attempted.

(C) Fortunately, the U.S. Navy had developed and was operating two general types of aircraft for anti-submarine warfare (ASW) operations; the S2 series of Grumman Tracker aircraft and the larger P2 series of Lockheed Neptune aircraft. It was also learned that the Naval Air Development Center (NADC), Johnsville, Pennsylvania, was operating S2-E aircraft that had been subjected to additional magnetic cleaning and were equipped to function as test beds for new magnetic detection systems. A joint AFCRL-NADC flight test program was initiated and arrangements completed to test the ARMS against land targets in the areas analogous to Southeast Asia and to make the system available for submarine detection tests in normal Navy operational areas.

5.2 Aircraft Installation

(C) A Grumman S2-E Tracker aircraft was especially modified for a series of land-target tests. The extendable boom system was mated with the ARMS sensor, and the control and display panels were mounted in the right-hand ASW operator's position. Figure 8 shows the S2-E Aircraft with the boom extended, and Figure 9 shows the control and display panels installed in the aircraft. A four-track, magnetic, tape recorder; a dual trace, strip chart recorder; and an NADC land target filter package were also installed. Tape recordings were made of all flight operations with separate tracks assigned to the unfiltered, discriminated magnetometer output; the ARMS bandpass filter output; the NADC land target filter output; and a voice channel containing target heading, velocity and other pertinent data. In addition to the CRT trace displays, the ARMS and NADC filter outputs were recorded on the dual trace strip chart providing visual information for both MAD operators. In addition to normal bandpass functions, the NADC filter was constructed to provide adjustable rolloff at the edges of the selected pass band. Figure 10 shows the strip chart recorder, the nine-term compensator, and general appearance of the left side ASW operator's position.

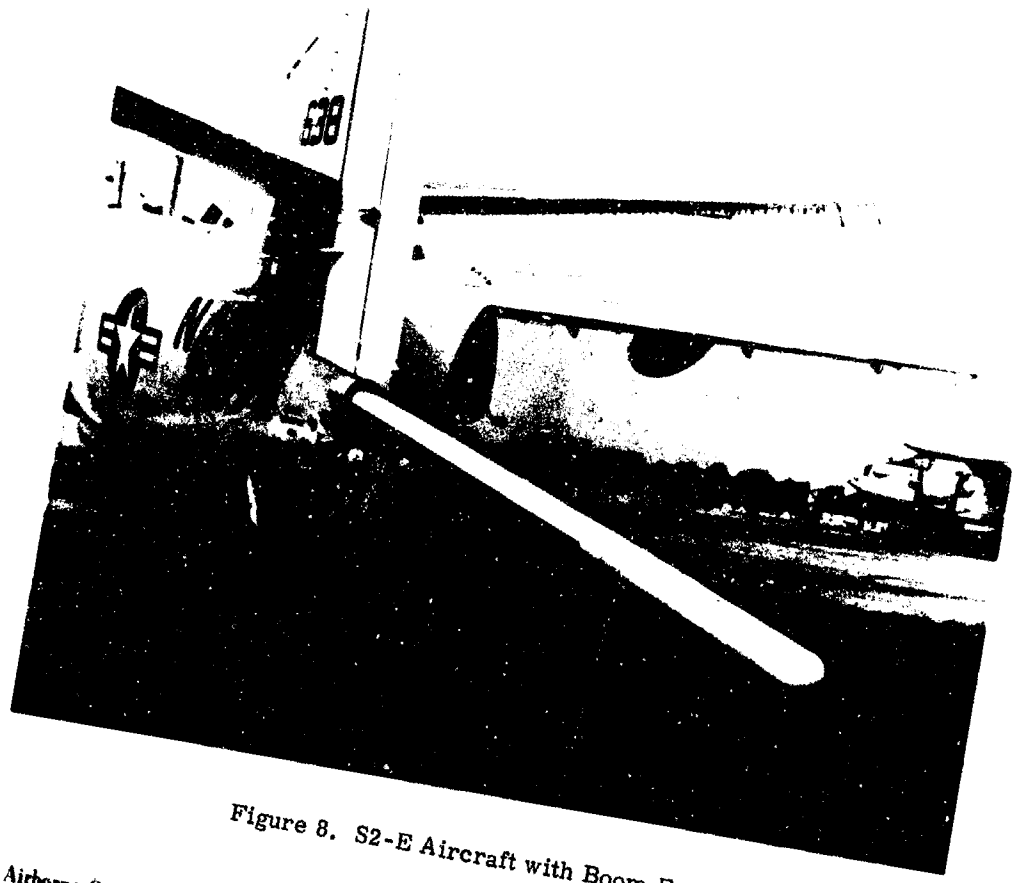

Figure 8. S2-E Aircraft with Boom Extended

5.3 Airborne Operations

(U) The flight test program involved four distinct operational areas: the Florida Keys (NAS, Key West), the southern coastal plain and south central Georgia (NAS, Glynco), the southern Blue Ridge area of the Appalachians, the Appalachian Piedmont of North Carolina (Pope AFB and Sewart AFB), and the Mississippi Delta and alluvial plains section of Louisiana (NAS, New Orleans). Except for Key West, chosen for its low background noise levels, each area was analogous to a portion of Southeastern Asia. Target vehicles were used in Florida and Georgia, but as the balance of the tests were concerned with background noise levels only, targets of opportunity were utilized. Figure 11 is a plot of signal strength in gammas vs. distance for 1-1/2 and 2-1/2 ton trucks at the geomagnetic latitude of Florida assuming that the detector passes over or nearly over the target and that the trucks are heading in a north or south direction.

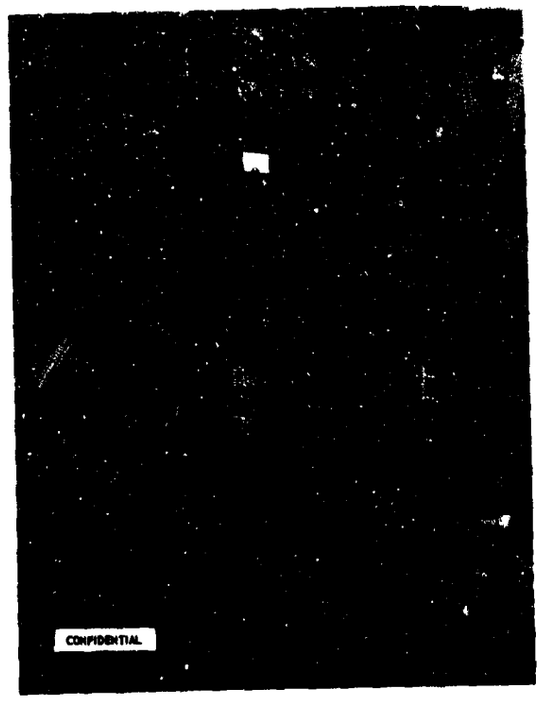

Figure 9. Control and Display Panel Installation

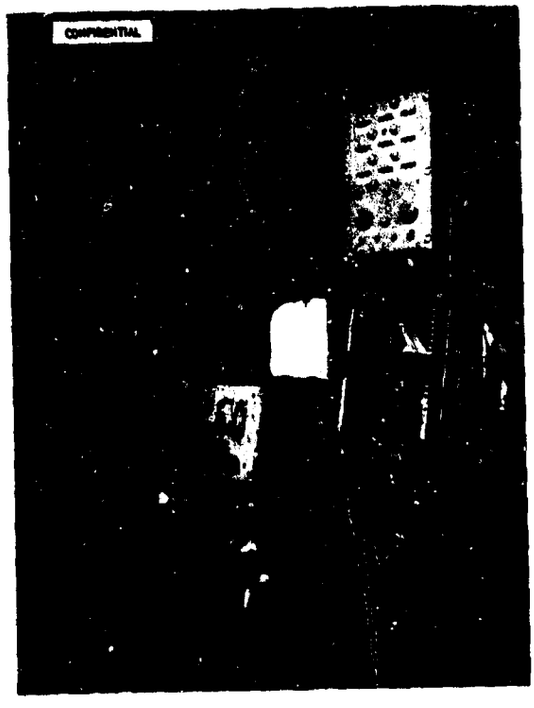

Figure 10. Recorder and Compensator Installations

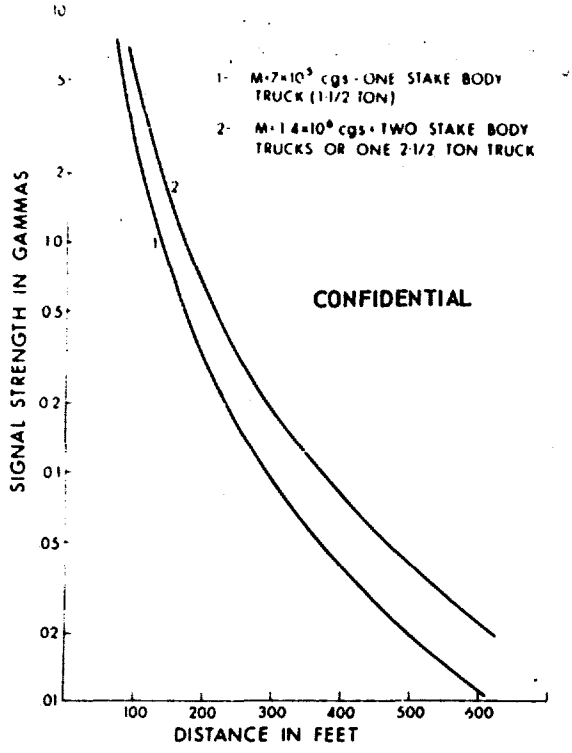

Figure 11. Signal Strengths vs. Distance for 1-1/2 and 2-1/2 Ton Trucks

5.3.1 FLORIDA KEYS

(S) The collection of aeromagnetic signatures began in the Key West, Florida area in June 1968. The aircraft was operated from NAS, Key West, and the target vehicles were located on the north end of Torch Key. The geologic noise level over the coral bedrock was generally less than 0.05γ for the filter band pass of 0.07 to 0.5 Hz and altitudes from 100 to 300 feet. The absence of dwellings and power lines kept interference at a minimum and occasional noise spikes could be related to the buried and underwater remains of the overseas railway. It should be noted that the low-level noise tests were in accord with systems checks performed at 5500 feet over NADC, Johnsville, just prior to data collection in Florida. These tests showed a noise level of 0.03γ for straight and level flight and a similar band-pass setting. Natural noise (ionospheric, solar, etc.) was estimated to be responsible for about 0.01 to 0.02 gamma during the Florida tests and the salt water-land interface was also responsible for a small noise contribution.

(C) One and one-half ton, stake-body, trucks were selected as primary target vehicles because of their similarity to ordinary farm vehicles of the type used to move supplies in disputed areas. Component ground measurements showed that

their maximum magnetic moments occurred when facing north. Representative values for two such trucks were 7.25 and 6.83 · 10^5 cgs units and for a standard station wagon, also used as a target, a value of 6.70 · 10^5 cgs was obtained.

(S) Passes were made over the target area using a modified cloverleaf ASW pattern with four passes on either the cardinal or intercardinal headings per pattern. A total of more than 50 such patterns were completed over a variety of targets. Figure 12 shows signatures obtained in Florida over a single target vehicle and Figure 13 shows additional test results in Florida and Georgia. Operating under the very favorable conditions of the Florida Keys area, we could detect a single stake-body truck pointing in any direction with the aircraft making an overhead pass on any heading at target distances of 400 feet. With a favorable truck heading, generally north, and with passes north or south, a single

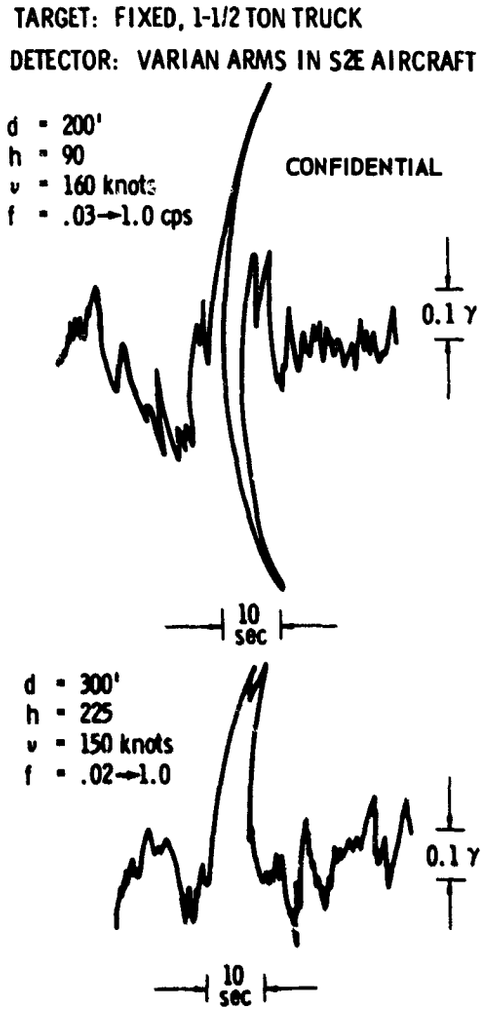

Figure 12. Flight Signatures - Single Target

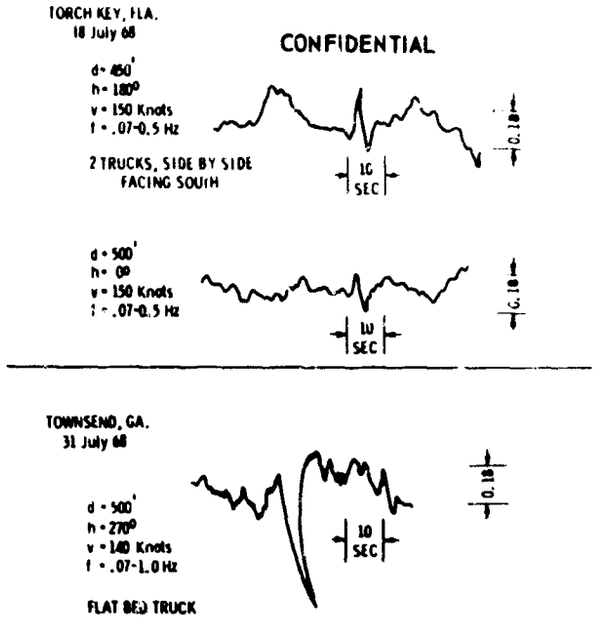

Figure 13. Flight Signatures - Multiple Target

truck could be found at distances between 500 and 600 feet. A standard station wagon also showed similar results. A truck park containing two stake-body trucks, a station wagon, and a sedan could be detected at 600 feet for any combination of heading and pass direction and at 800 feet for the more favorable ones. Tests were also conducted with the aircraft passing to the side of the target area and as expected all results were consistent with the geometry of the dipole signature pattern. Figure 14 is a theoretical plot of signature frequency vs. altitude and ground speed. It was observed that the combined effects of filters, pen amplifiers, and pen-paper friction increased the observed signal period. Best results were obtained using a filter bandpass of 0.07 to 1.0 Hz. A setting of 0.07 to 0.5 Hz was also particularly useful for the longer range signals. If a fixed filter is required for operations against land targets, the recommended setting at 120 knots is 0.07 to 0.7 Hz.

5.3.2 GEORGIA

(U) The Atlantic coastal plain of Georgia is analogous to the coastal plains of Southeast Asia and also similar to their peninsular plains and uplands. The Thailand portion of the Malay Peninsula, the Andaman Sea Coast of Thailand and its eastern coast on the Gulf of Siam are represented. The southwestern Cambodian coast, the Vietnam coast along the China Sea between the Mekong and Red River Deltas and the Tonkin Coast north from the Red River Delta to the Chinese border

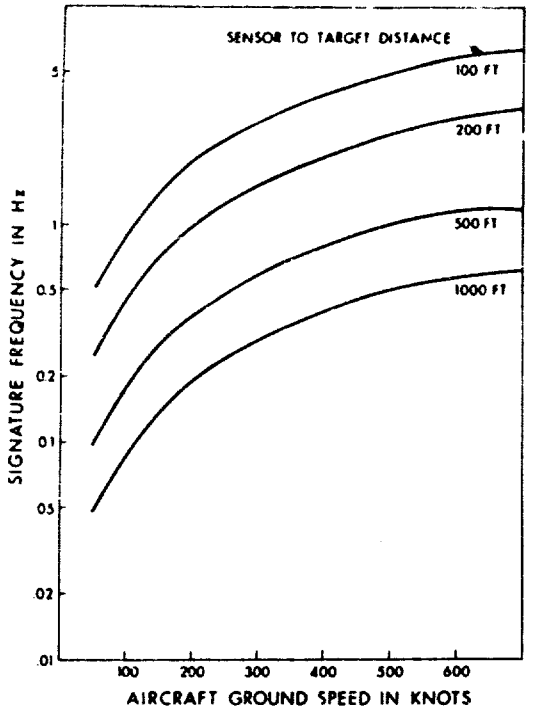

Figure 14. Signature Frequency vs. Altitude and Ground Speed

are well represented by this area. Like its Asian counterparts, the width of the plains varies from about 25 to 50 miles and includes low wet lands, sand and sand dune strips, some swampy forests, clay and silty soils and, alluvium underlain by marine sandstones. Two distinct operations were carried out in the plains area: a series of target detection passes; secondly, a low-level coastal overflight.

(S) Target detection operations were conducted at the Townsend, Georgia bombing range in a pine forested area broken by occasional grass and swamp lands. The natural geologic noise level was low (mostly less than 0.05γ), but power lines on the edge of the area, sentry posts, and the debris of many practice bombing missions gave strong signals when overflown. With a target consisting of two stake-body trucks parked side-by-side, signals with a S/N ratio of 3 or greater were obtained for overhead passes at altitudes up to 400 feet and for passes 200 feet to the side and 300 feet above.

(S) Changing the target to a single truck reduced range as expected. Overhead passes at 300 feet and a filter bandpass of 0.07 to 1.0 Hz produced S/N ratio equal to or less than 3 and at 400 feet S/N ratio dropped to approximately 2. Reducing the filter bandpass to 0.5 to 1.0 Hz resulted in the loss of all signal. It was estimated that a bandpass of 0.1 to 0.7 Hz would have been optimum. Additional passes at 500 feet and at 600 feet did not provide an identifiable signal.

(S) The coastal overflight originated at Brunswick, then went north to near Savannah, southwest to Alma, south to Waycross, over the Okefenokee Swamp to Lake City, Florida, and then returned to Brunswick. Altitude above ground was held at 300 feet throughout the flight and a filter bandpass of 0.07 to 1.0 Hz was used. Geologic noise levels were very low, levels of less than 0.05 gamma peak-to-peak being observed for long periods of time. Virtually all discernible signals could be correlated to man-made ground structures. Examples of objects with strong signals seen at the 300 foot level include barges, houses, rail tracks, bridges, trucks, and cars. Noise levels in the vicinity of Waycross dropped to 0.03γ, then to 0.02γ over the swamps and for most of the return trip to Brunswick. One section between Brunswick and Savannah had a noise level between 0.005 and 0.01γ for several minutes. Detection distances for a single truck would exceed 400 feet in these areas.

(S) The second analogous area studied during the Georgia operations in July and August 1968 was the Tifton Upland which corresponds to the Khorat Plateau of northeastern Thailand and western Laos. It is characterized by elevations of about 500 feet, gentle local relief, and wide, flat-bottomed valleys. Soils are sandy loams to sands with some oxidized iron, and the area is underlain with sedimentary rock. The flight passed over Alma, Douglas, Fitzgerald, Tifton, Nashville (Georgia), Willacoochee and returned to Douglas. Typical noise levels ran from 0.06 to 0.10γ for 0.07 to 1.0 Hz bandwidth and were directly attributable to local geology. Changing the bandpass to 0.5 to 1.0 Hz removed most of the geological effects as did climbing to higher altitudes. Maximum single-truck detection range in this area would be about 300 feet.

5.3.3 THE APPALACHIANS

(U) The southern Blue Ridge area of the Appalachians is similar to the major mountain range of southeastern Asia, the Chaine Annamitique. This range runs through central and southern Laos, the southern portion of North Vietnam, the northern portion of South Vietnam and the eastern one-fourth of Cambodia. Like its Asian counterpart, the area contains mountains characterized by long narrow ridges and valleys and is often heavily dissected. The relief is very pronounced and the geology complex containing granitic and basaltic intrusives. Elevation varies from 2500 to 6500 feet and the prevailing soil is a clayey silt underlain with an iron-rich laterite.

(S) This area was most difficult to fly due to its sharp relief and high peak altitudes, and it was the most disturbed magnetically. It was also an almost exact duplicate of much of the area traversed by sections of the Ho-Chi-Minh Trail. Operating out of Pope AFB, Fayetteville, North Carolina, the flight tests for this section began just west of Winston-Salem at altitudes of 200 to 300 feet above ground.

Noise levels for the 0.07 to 1.0 Hz pass band often exceeded 1γ, sometimes reached 2γ, and on a few short sections, soared to 10γ. The mountain valleys, stream beds, and hollows showed average noise levels of 0.1 to 0.2γ with the best results obtained along the edges of the mountain lakes.

(S) Detection range for a single truck averaged around 200 feet dropping to 150 feet or less in the more noisy areas. Also note that the violent aircraft maneuvers necessary to maintain ground clearance added to the overall noise. One type of readily observable target often noted in this area was the small steel highway bridge, often only one lane wide, used to cross the many streams in the area. Large drainage culverts placed under dirt farm access roads also were noted along with water tanks and towers.

(S) Proceeding westward toward Sewart AFB, Tennessee, a short test line was recorded across the Cumberland Plateau. Elevations range from 1600 to 2000 feet with local relief generally less than 100 feet. This section is analogous to the Shan Highlands of east-central Burma and although not of immediate concern is of possible future significance. Observed noise in this area was about 0.1γ rising to 0.2γ occasionally and dropping to 0.05γ. Good signals were readily obtained from trucks, farm buildings, sheds, and grain silos.

(S) The Appalachian Piedmont of North Carolina was the next area tested. It is similar to the basaltic plateaus of the Chaine Annamitique and is representative of the gently rolling to hilly terrain. Pleiku and Dak Song lie on such plateaus and are underlain with granites and basalts, respectively. Albermarle, North Carolina, is typical of the general region. Elevation is less than 1000 feet and relief between valley bottoms and crests is 100 to 200 feet. Soils are silt-loams and gravelly silt-loams mixed with slaty gravel, and the area is underlain with metamorphosed, volcanic rock. Flight lines in this area passed through or near to Albermarle, High Point, Sanford, and Wadesboro. The average noise level within the target passband lies between 0.4γ and 2γ indicating a detection range of about 150 feet. The local geology was the limiting factor, but it should be noted that the area is not uniformly bad and detection at twice the above range would occasionally be possible.

5.3.4 MISSISSIPPI RIVER

(U) The fourth test area included the Mississippi Delta section of Louisiana and the Mississippi River alluvial plain section of Mississippi. The delta section is analogous to the deltas of Southeast Asia, including the Mekong River Delta in Cambodia and South Vietnam, and the Red River Delta in North Vietnam. Elevations are less than 25 feet above sea level and both natural and artificial levees are prevalent. Extensive marshes and tidal swamps are common. Clays and silts predominate and are underlain with alluvial sediments of great thickness. The base of operations for flights in this area was NAS, New Orleans.

(S) The flight path for the Delta tests began just south of New Orleans, passed eastward over Lake Borgne to Ship Island, then south to South Pass, and then west via Southwest Pass, Timbalier Bay, and Point Au Fer Island. A series of east-west passes at various levels were flown over the area and then a single northeastward pass returned the aircraft to New Orleans. Noise levels were higher than predicted. At 300 feet and a bandpass of 0.07 to 0.5 Hz noise levels averaged about 0.2γ. Opening the bandpass to 1.0 Hz did not increase the background noise, but the observed long period noise (10 to 20 seconds) suggests that a filter with a low pass above 0.1 Hz could reduce noise by a factor of 2. Tests in this area were complicated by navigation aids such as beacons, lights and buoys, and by drilling platforms, pipe lines and completed oil and gas wells. Many of these objects produced signals strong enough to saturate recorders at distances over 1000 feet. Near Grand Isle, on the southern Louisiana coast, noise levels dropped to 0.1γ briefly, and small work boats used to ferry workers between docks and drilling platforms could be detected at 300 feet.

(U) The alluvial plain section of the Mississippi runs from the southern tip of Illinois to the delta section and is confined to a narrow river valley sharply defined by hills to the east. It is similar to the inland plains of Thailand and Cambodia and to small areas of the Red River in North Vietnam near Hanoi. The soils are silty and plastic clays over deep sedimentary beds, elevations range from 100 to 300 feet, and relief is gentle. Proceeding north from New Orleans, the survey aircraft flew from Baton Rouge to Natchez along the river bed frequently crossing the many twists of the Mississippi River and returning over a similar route. Flight altitude varied from 200 to 400 feet, occasionally going higher to avoid bridge and cable crossings.

(S) Noise levels continued to be a little higher than anticipated running from 0.15γ to 0.3γ. Results were similar to the delta area flights and indicated that the filtering of some of the longer period geologic noise could be accomplished without much loss of signal. It was observed that the strings of barges used to transport bulk liquids on the river could be detected at distances of over two thousand feet and that the smaller tugs or motorized barges produced saturating signals at over five hundred feet. Almost any kind of steel vessel of sufficient size to navigate on the river could be detected at over 400 feet.

6. SIGNAL CONDITIONING

(U) The magnetic tapes and strip charts accumulated during flight tests were subjected to preliminary processing at NADC, Johnsville. Schneider (1969) investigated maximum slant detection range in terms of the operator's ability to recognize

SECRET

(This page is confidential)

a signal in the noise background. A recognition scale factor (RSF) was assigned to each recorded signal with 0 representing a signal indistinguishable from the noise and 10 representing a high intensity signal at least five times larger than background noise. Data collected over Torch Key was plotted as peak-to-peak signal intensity versus RSF and the following expression was derived for RSF from these plots

$$RSF = \frac{S - 0.25N + 0.083}{0.54N + 0.022} \qquad (4)$$

where S = peak-to-peak signal level in gammas, and

N = peak-to-peak noise level in gammas.

An RSF of five is considered the minimum signal that can be recognized by the average operator without prior knowledge of the target location. An operator with some knowledge of a possible target location can recognize more difficult signals, possibly down to an RSF of three. Plots were prepared of the frequency of detection versus aircraft altitude (slant range) for signals possessing an RSF of at least three. Figure 15 shows such a plot for a target consisting of two 1-1/2 ton, stake-body trucks parked side by side.

(C) A limited effort was made to process the signal data to improve the signal-to-noise ratio. The first step consisted of filtering the data to diminish the signal amplitude of the longer range subsurface noise sources without reducing the target signal amplitudes. If the magnitude of the noise signal remained of the same order as the target signal, then the field rate of change was used for signal-to-noise discrimination. Figure 16 shows the results of such a signal enhancement process. The upper trace was recorded in the normal manner through a filter setting of 0.07 to 0.5 Hz. The target was a single stake-body truck heading east and the aircraft passed overhead at 400 feet on a north heading at 148 knots. The lower trace, recorded with the same scale factors, is the result of rate limiting the upper signal and subtracting the resultant from the original. It is estimated that the real time application of such a procedure could increase slant detection range 30 - 35 percent.

7. ANALYTICAL INVESTIGATIONS

(U) Concurrently with the experimental program, an analytical investigation of target signatures was pursued. The purpose was to determine how the characteristics of target signatures such as amplitudes, frequencies, and wave forms changed with various parameters such as (1) orientation of the dipole, (2) aircraft altitude, (3) heading of the aircraft, and (4) with distance of nearest approach.

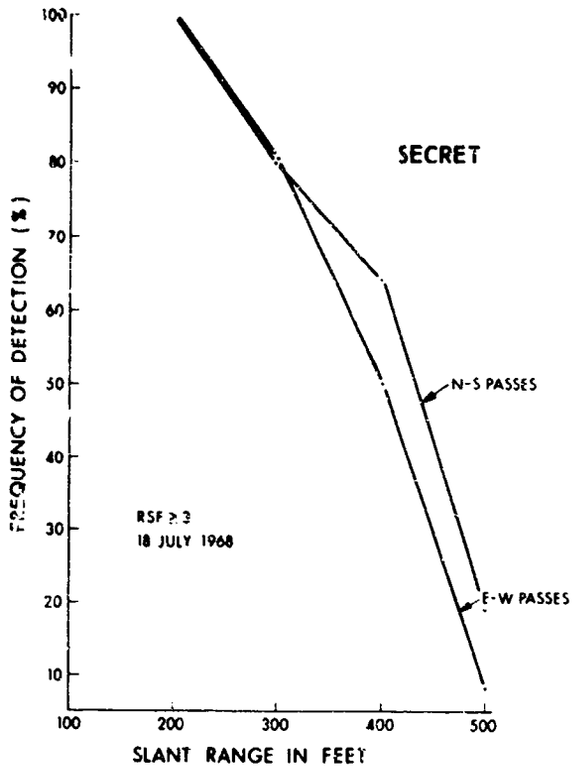

Figure 15. Frequency of Detection vs. Slant Range for RSF $\geq$ 3

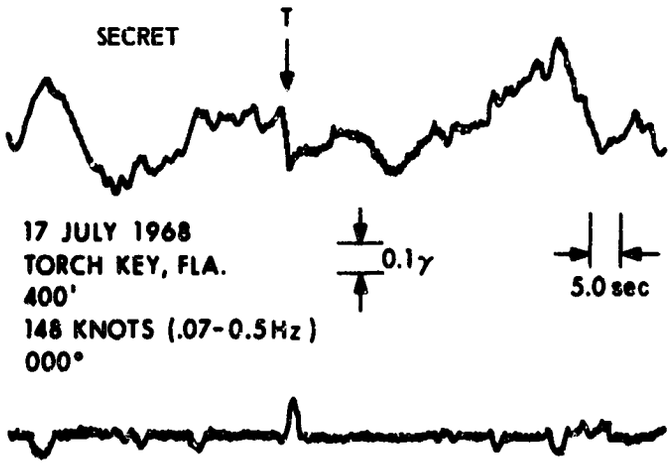

Figure 16. Signal Enhancement by Rate Limiting and Subtraction

SECRET

(This page is unclassified)

(U) The equations of the components of the magnetic signature for a flight past a dipole-type target were derived and are given below

$$B_x = \frac{M}{r^4}\left[2x\cos\theta + \frac{1}{r}\left\{y(x\cos\beta - y\cos\alpha) - z(z\cos\alpha - x\cos\gamma)\right\}\right] \quad (5)$$

$$B_y = \frac{M}{r^4}\left[2y\cos\theta + \frac{1}{r}\left\{z(y\cos\gamma - z\cos\beta) - x(x\cos\beta - y\cos\alpha)\right\}\right] \quad (6)$$

$$B_z = \frac{M}{r^4}\left[2z\cos\theta + \frac{1}{r}\left\{x(z\cos\alpha - x\cos\gamma) - y(y\cos\gamma - z\cos\beta)\right\}\right] \quad (7)$$

where M is the magnitude of the dipole moment of the target and where

$$r = \left(x^2 + y^2 + z^2\right)^{1/2} \quad (8)$$

and is the distance from the target to the point P (x, y, z) at which the field is being measured. The direction cosines of the target dipole moment are cos α, cos β, and cos γ. Theta is the angle between the vectors $\vec{M}$ and $\vec{r}$. Therefore,

$$\cos\theta = \frac{\vec{M}}{\sqrt{\vec{M}\cdot\vec{M}}} \cdot \frac{\vec{r}}{\sqrt{\vec{r}\cdot\vec{r}}} \quad (9)$$

$$\text{or } \cos\theta = \frac{x\cos\alpha + y\cos\beta + z\cos\gamma}{(x^2 + y^2 + z^2)^{1/2}} \quad (10)$$

(U) The quantity sensed by the detector is approximately equal to the projection of the target's magnetic field onto the ambient earth's field. A digital computer program was written to calculate target signatures. A sequence of profiles of the magnitude of a target field for different aircraft headings and at an altitude of 200 feet with an off-set distance of 287 feet is illustrated in Figure 17. The distance of nearest approach for each of these signatures was 350 feet. Figure 18 shows how the target signature varies as the offset distance increases while the aircraft heading and altitude are kept constant (heading = 90 degrees, altitude = 200 feet). The offset distance is the horizontal distance between the target and the ground track of the aircraft. Notice that the target pulse actually inverts itself. The orientation of the dipole moment used in calculating the signatures shown in Figures 17, 18, and 19 was in a north-south plane with a dip angle of 45 degrees. The dip angle of the earth's field used in the calculations was that measured at Key West, Fla., 57.1 degrees. The dipole moment was 7×10^5 emu. Because of the inclination of the target dipole moment, the signatures are not symmetrical with

SECRET

(This page is unclassified)

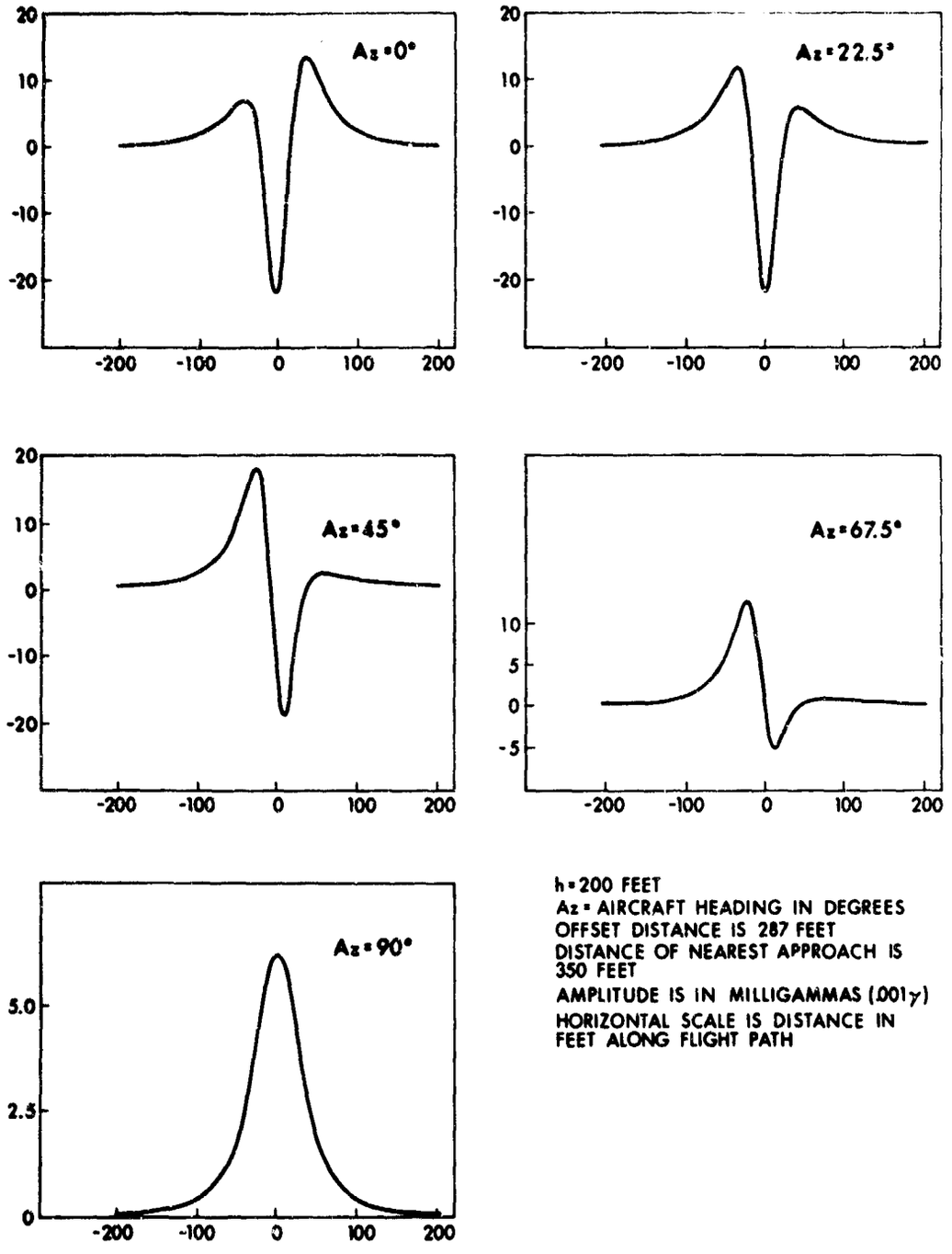

Figure 17. Target Amplitude vs. Aircraft Heading

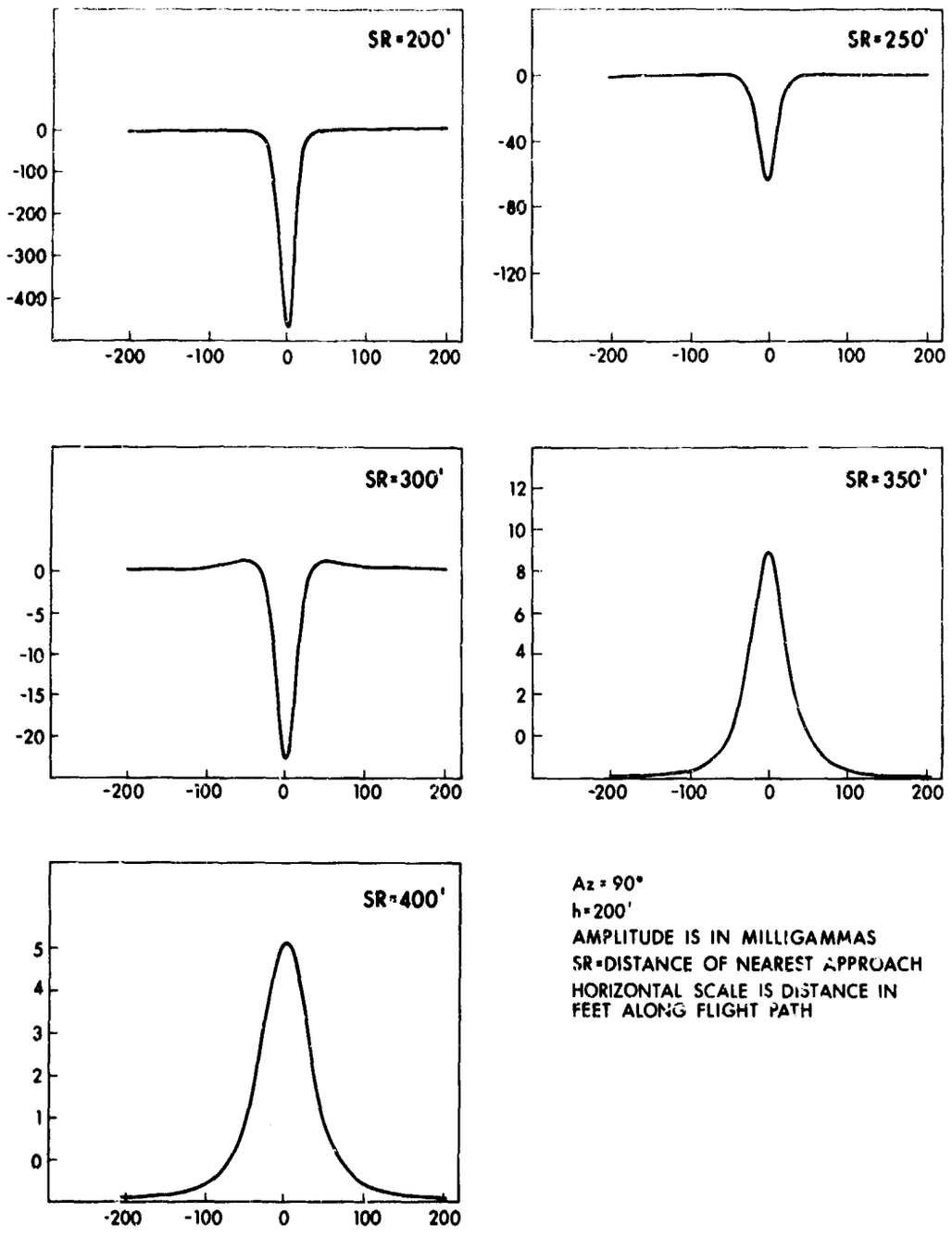

Figure 18. Target Amplitude vs. Slant Range

respect to the target position assuming that the signature is calculated along a constant altitude flight path. An example of the asymmetry of the target signatures is shown in Figure 19.

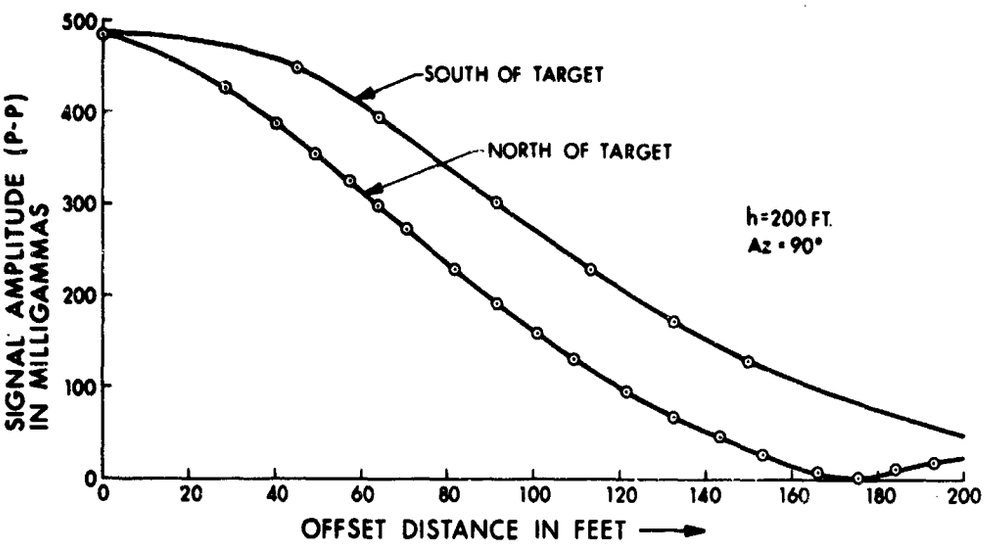

Figure 19. Target Amplitude vs. Offset Distance

(U) The target signal is passed through a bandpass filter in order to eliminate magnetic noise due to aircraft maneuvers, local geological formations, and ionospheric disturbances. The effect of the bandpass filter is to attenuate the high and low frequency components inherent in the target signature as well as to attenuate the magnetic noise. Therefore, the experimentally measured filtered signal can not be validly compared to the analytically calculated signature directly. To make the results more comparable one must (1) calculate the power spectrum of the target signal, (2) attenuate the various frequencies in accordance with the requirements of the bandpass filter, and finally, (3) reconstruct the modified target signal from the attenuated power spectrum. By such a procedure, one should get a valid comparison between theory and experiment provided that the magnetic noise is negligible. However, in the more realistic case, the magnetic noise is a serious problem which must be eliminated by narrowing the bandpass filter settings at the expense of attenuating the target signal.

(C) A number of power spectra of target signatures were calculated. Most of the time they had a peak at approximately 0.01 Hz or less. The amplitude of the power spectra at frequencies greater than 0.1 Hz is approximately one percent of

peak amplitude. From an examination of the power spectra, it is evident that the lower limit of the bandpass filter should be set as low as possible consistent with eliminating undesirable magnetic noise in order that the target signal be attenuated as little as possible. A lower upper limit would also seem permissible. These recommendations refer to the 0.07 - 1.0 Hz bandpass filter limits used in the experimental flight tests. However, in the final analysis these filter-limit settings must be determined experimentally because the local noise conditions may be a dominating factor that must be taken into consideration.

(C) Figure 20 shows a comparison between the unfiltered components of the magnetic signature of a 3/4-ton Army weapons carrier as measured by the Sharpe magnetometer on the ground and calculated curves utilizing Eqs. (5), (6), and (7). The calculated results were normalized both in phase and magnitude only at the peak of the z-component curve. The x- and y-component curves are out of phase with the experimental values. This may be largely due to the possibility that points chosen on each of the measured component curves were not coincident in time. Of course, if each component curve was normalized separately with respect to phase much better agreement would result.

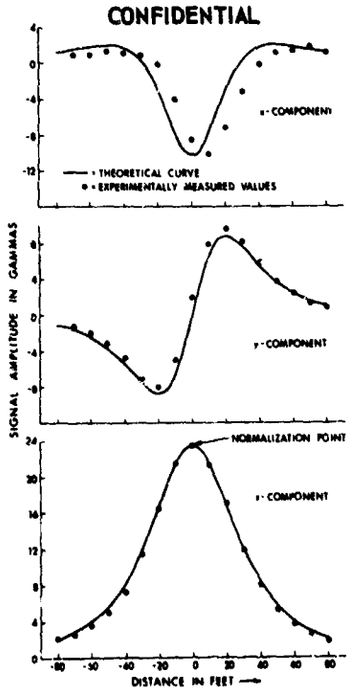

Figure 20. Theoretical vs. Experimental Signatures

(U) It may be necessary to calculate the magnetic signature of a group of vehicles as might be found in a parking area or supply convoy. This can be done analytically in a straightforward manner by generalizing the earlier equations for a single dipole.

(U) Assume that there are N vehicles present. Let the coordinates of the i^{th} vehicle be x_i, y_i, and z_i, and let the dipole moment, M_i, of this vehicle have direction cosines given by $\cos \alpha_i$, $\cos \beta_i$ and $\cos \gamma_i$. The x-component of the resultant field is given by

$$F_x = \sum_{i=1}^{i=N} F_{xi} \tag{11}$$

where

$$F_{x_i} = \frac{M_i}{(r - r_i)^4} \left[2(x - x_i) \cos \theta_i + \frac{1}{(r - r_i)} \left\{ (y - y_i) \left\{ (x - x_i) \cos \beta_i \right.\right.\right.$$

$$\left.\left.\left. - (y - y_i) \cos \alpha_i \right\} - (z - z_i) \left\{ (z - z_i) \cos \alpha_i - (x - x_i) \cos \gamma_i \right\} \right\} \right] \tag{12}$$

$$|r - r_i| = \left\{ (x - x_i)^2 + (y - y_i)^2 + (z - z_i)^2 \right\}^{1/2} \tag{13}$$

$$\cos \theta_i = \frac{\vec{M}_i}{M_i} \cdot \frac{\vec{r} - \vec{r}_i}{|\vec{r} - \vec{r}_i|} \tag{14}$$

and $\vec{r} = x\hat{i} + y\hat{j} + z\hat{k}$ (15)

and similarly for the y and z components.

8. CONCLUSIONS

(S) An airborne reconnaissance magnetometer system (ARMS) installed in a suitably compensated and boom-equipped aircraft is an effective device for locating targets containing large amounts of ferromagnetic materials. Its applicability to and its usefulness in most of SEA has been demonstrated through test flights in the United States over analogous geologic and geographic areas. The system is capable of locating trucks, steel pontoon bridges, gun and radar emplacements, fuel tanks, and many other similar targets at ranges of several hundred feet. Larger targets such as steel bridges, boats, and barges could be detected at up to two thousand feet.

(S) Detection range for a single farm-type truck under good operating condition would be about 400 feet and the addition of a real time, inflight data processor could increase this to more than 500 feet. Large fleets of native craft or groups of dwellings could be interrogated quickly and those units containing significant amounts of metal in the form of engines, weapons, or supplies marked by dyes or flares for investigation and possible destruction. Table 7 summarizes our findings.

(U) Table 7. Aeromagnetic Detection Summary

Advantages	Disadvantages
Passive	Limited Range
All Weather	Subject to Geologic Noise
Non-jammable	Subject to Ionospheric Noise
Unaffected by Foliage	High Per Unit Cost
Real Time Display	Compensated Aircraft Required

(C) It can also be concluded from the good agreement shown between the analytical and experimental results that the equations presented are valid and therefore can be used to predict target signatures accurately. Appendix A explains equation derivations.

9. FUTURE PROGRAMS

(C) Two new aircraft will soon be available to the Navy for their ASW program: the twin jet S-3A and the longer range P-3C. It is anticipated that the S-3A will provide better detector-noise background. Because of its greatly increased speed, it could provide a better signal-to-noise ratio in many areas of operation. It would also be less vulnerable to ground fire.

(C) No improvements in instrument sensitivity are foreseen in the near future but systems weight and warm-up time could be reduced. Filter selection could be optimized for specific areas and types of targets and real time signal processing equipment could be test flown.

Acknowledgments

The assistance of the scientific and flight personnel of the Naval Air Development Center, Johnsville, Pennsylvania, and of the Navy and Air Force bases from which operations were conducted is gratefully acknowledged. Special thanks are given to Mr. Elwood Maple for his careful review of technical content, his verification of computations, and for his many helpful suggestions.

References

Curtis, C. E. (1966) Terrain Analysis and Related Studies within Tropic Environments: Southeast Asian Region, Surinam, and the Mali Republic, Final Report, Contract AF19(628)-4166.

Fisher, R. S. (1966) Detection of Buried Ferrous Objects and Earth Voids in Thailand Using the Rubidium Vapor Magnetometer I, II, Military R + D Center, Bangkok, Thailand.

Flannery, W. T., Buchanan, M. T., Roberts, G. F., and Morris, F. J. (1967) A Feasibility Study of a Component Gradiometer, AFCRL-67-0417.

Johnston, M. J. S. and Stacey, F. D. (1968) Magnetic disturbances caused by motor vehicles and similar ferrous bodies, J. Geomag. and Geoelec., 20, No. 1.

Maple, E. (1966) Aerial Magnetic Detection in Counter-Insurgency Warfare - A Preliminary Technical Report. Air Force Surveys in Geophysics, No. 172.

McBride, R. A. (1967) Airborne Reconnaissance Magnetometer System, Final Report, AFCRL 67-0694, Contract AF19(628)-67-C-0144.

References

McBride, R. A. (1968) Airborne Reconnaissance Magnetometer System, Supplement to the Final Report, AFCRL 68-0359, Contract AF19(628)-67-C-0144.

McClay, J. and Shuman, B. (1965) Magnetic Compensation of Aircraft, AFCRC-TR-56-206.

Schneider, R. J. (1969) Test of the ARMS (Airborne Reconnaissance Magnetometer System) for Detection of Land Targets, Secret Report, NADC.

Appendix A

Equation Derivations

(U) Assume that an arbitrarily orientated dipole is located at the origin of a coordinate system. The x-y plane is intended to be coincident with the ground and the z-axis is positive in the upward direction. Our problem consists of determining the equations for the components along an arbitrary level flight path past the dipole. Let the direction cosines of the dipole moment be cos α, cos β, and cos γ and let the point P (x, y, z) be an arbitrary point along the flight path. The position vector of the point P (x, y, z) is given by

$$\vec{r} = x\hat{i} + y\hat{j} + z\hat{k} \tag{A1}$$

where $\hat{i}$, $\hat{j}$, and $\hat{k}$ are the usual unit vectors along the positive x, y, and z axes. The dipole moment vector is given by

$$\vec{M} = M(\cos\alpha\hat{i} + \cos\beta\hat{j} + \cos\gamma\hat{k}) \tag{A2}$$

The potential at a distance r from a magnetic dipole large compared to its length is

$$V = \frac{\vec{M} \cdot \vec{r}}{r^3} = \frac{M}{r^2}\cos\theta \tag{A3}$$

where θ is the angle between $\vec{r}$ and $\vec{M}$ and the magnetic induction, $\vec{B}$, due to the moment $\vec{M}$ is the negative of the gradient of the magnetic potential or

$$\vec{B} = -\vec{\nabla} V \tag{A4}$$

$$\text{Hence } \vec{B} = -\left(\hat{i}\frac{\partial}{\partial x} + \hat{j}\frac{\partial}{\partial y} + \hat{k}\frac{\partial}{\partial z}\right)\left(\frac{\vec{M}\cdot\vec{r}}{r^3}\right) \tag{A5}$$

Carrying out the operation of Eq. (A5) yields

$$\vec{B} = \frac{1}{r^3}\left\{\frac{3(\vec{M}\cdot\vec{r})\vec{r}}{r^2} - \vec{M}\right\} \tag{A6}$$

Since the component of the target field which is perpendicular to the earth's field makes a completely negligible contribution in the detected signal, we can say that the field sensed by the detector is approximately equal to the projection of the target's magnetic field onto the ambient earth's field. The error in this approximation will be less than one percent. The measured target signal B_s will therefore be given by the dot product of Eq. (A6) with a unit vector in the direction of the earth's field (F).

$$B_s = \vec{B}\cdot\hat{F} \tag{A7}$$

$$B_s = \frac{1}{r^3}\left\{\frac{\vec{M}\cdot\vec{r}}{r^2}(\vec{r}\cdot\hat{F}) - \vec{M}\cdot\hat{F}\right\} \tag{A8}$$

An expanded form of Eq. (A8) was used to calculate target signatures.

(U) If we expand Eq. (A6) we get the following expression for the x-component of the target field:

$$B_x = \frac{M}{r^3}\left\{\frac{3x\,(x\cos\alpha + y\cos\beta + z\cos\gamma)}{r^2} - \cos\alpha\right\} \tag{A9}$$

$$B_x = \frac{M}{r^4}\left(3x\cos\theta - \frac{r^2\cos\alpha}{r}\right) \tag{A10}$$

$$B_x = \frac{M}{r^4}\left\{2x\cos\theta + x\cos\theta - \frac{(x^2+y^2+z^2)\cos\alpha}{r}\right\} \tag{A11}$$

but

$$x\cos\theta = \frac{x}{r}(x\cos\alpha + y\cos\beta + z\cos\gamma) \tag{A12}$$

$$\therefore \frac{1}{r}(xr\cos\theta - r^2\cos\alpha) = \frac{1}{r}(x^2\cos\alpha + xy\cos\beta + xz\cos\gamma$$

$$- x^2\cos\alpha - y^2\cos\alpha - z^2\cos\alpha) \qquad \text{(A13)}$$

$$= \frac{1}{r}\Big\{ y(x\cos\beta - y\cos\alpha)$$

$$- z(z\cos\alpha - x\cos\gamma)\Big\} \qquad \text{(A14)}$$

Substituting the right hand member of Eq. (A14) into Eq. (A11) yields

$$B_x = \frac{M}{r^4}\left[2x\cos\theta + \frac{1}{r}\Big\{y(x\cos\beta - y\cos\alpha) - z(z\cos\alpha - x\cos\gamma)\Big\}\right] \qquad \text{(A15)}$$

which is Eq. (5), the equation we set out to derive. Equations for B_y and B_z can be derived in a similar manner.

SECRET

Unclassified
Security Classification

DOCUMENT CONTROL DATA - R&D

(Security classification of title, body of abstract and indexing annotation must be entered when the overall report is classified)

1. ORIGINATING ACTIVITY (Corporate author) Air Force Cambridge Research Laboratory (CRF) L. G. Hanscom Field Bedford, Massachusetts 01730	2a. REPORT SECURITY CLASSIFICATION Secret 2b. GROUP 3

3. REPORT TITLE
AERIAL MAGNETIC DETECTION IN COUNTER-INSURGENCY WARFARE - PART II, EXPERIMENTAL RESULTS

4. DESCRIPTIVE NOTES (Type of report and inclusive dates)
Scientific, Interim.

5. AUTHOR(S) (First name, middle initial, last name)
Edward J. Zawalick, Lt. Col. USAF (Retired)
Robert O. Hutchinson

6. REPORT DATE February 1970	7a. TOTAL NO. OF PAGES 47	7b. NO. OF REFS 9
8a. CONTRACT OR GRANT NO. b. PROJECT, TASK, WORK UNIT NOS. 7601-03-01 8601-06-01 c. DOD ELEMENT 62101F 61102F d. DOD SUBELEMENT 681000 681311	9a. ORIGINATOR'S REPORT NUMBER(S) AFCRL-70-0096 9b. OTHER REPORT NO(S) (Any other numbers that may be assigned this report) AFSG, No. 215	

10. DISTRIBUTION STATEMENT 2—This material contains information affecting the national defense of the United States within the meaning of the Espionage Laws (Title 18, U.S.C., Sections 793, 794) the transmission or revelation of which in any manner to an unauthorized person is prohibited by law.

11. SUPPLEMENTARY NOTES TECH, OTHER	12. SPONSORING MILITARY ACTIVITY Air Force Cambridge Research Laboratory (CRF) L. G. Hanscom Field Bedford, Massachusetts 01730

13. ABSTRACT

Component gradiometer and total intensity magnetometer systems performances for use in aerial magnetic detection were compared. Permanent and induced fields and resultant magnetic moments and the ranges of variations for target vehicles were obtained. Dynamic signatures from these same vehicles were obtained with a modified commercial magnetometer. The total field system was installed in a Grumman Tracker (S2E) aircraft and a joint program with the Naval Air Development Center, Johnsville, Pa., resulted in a series of flight tests over various combinations of target size, spacing, heading, and geologic conditions. Analytical expressions were derived for target signatures and showed good agreement with experimental values. Application of the observed results to specific areas within Southeastern Asia and their associated geologic noise spectra is discussed.

DD FORM 1 NOV 65 1473

Unclassified
Security Classification

SECRET

Unclassified

Security Classification

14. KEY WORDS	LINK A		LINK B		LINK C	
	ROLE	WT	ROLE	WT	ROLE	WT
Aerial Magnetic Detection Magnetometer Gradiometer Magnetic Moment Magnetic Field						

Unclassified

Security Classification